Supersonic Aerodynamic Characteristics of Monoplanar Missiles with Low-Profile Quadriform Tails

A. B. Blair Jr.*
NASA Langley Research Center, Hampton, Virginia 23665

Wind-tunnel tests were conducted on monoplanar circular missile configurations with low-profile quadriform tail fins to provide an aerodynamic data base to study and evaluate air-launched missile candidates for efficient conformal carriage on supersonic-cruise-type aircraft. The tests were conducted in the NASA Langley Unitary Plan Wind Tunnel at Mach numbers 1.70–2.86 for a constant Reynolds number per foot of 2.00×10^6. Selected test results are presented to show the effects of tail-fin dihedral angle, wing longitudinal and vertical location, and nose-body strakes on the static longitudinal and lateral-directional aerodynamic stability and control characteristics.

Nomenclature†

b = reference wing span, 0.8033 ft
C_D = drag coefficient, drag/qS
C_L = lift coefficient, lift/qS
C_ι = rolling-moment coefficient, rolling moment/qSb
C_{ι_β} = effective-dihedral parameter, $(\Delta C_\iota/\Delta\beta)_{\beta=0 \text{ deg, } 3 \text{ deg}}$
$C_{\iota_{\delta_{roll}}}$ = $\Delta C_\iota/\Delta\delta_{roll}$, per degree
$C_{\iota_{\delta_{yaw}}}$ = $\Delta C_\iota/\Delta\delta_{yaw}$, per degree
C_m = pitching-moment coefficient, pitching moment/$qS\iota$
C_{m_δ} = $\Delta C_m/\Delta\delta_{pitch}$, per degree
C_n = yawing-moment coefficient, yawing moment/qSb
C_{n_β} = directional-stability parameter, $(\Delta C_n/\Delta\beta)_{\beta=0 \text{ deg, } 3 \text{ deg}}$
$C_{n_{\delta_{roll}}}$ = $\Delta C_n/\Delta\delta_{roll}$, per degree
$C_{n_{\delta_{yaw}}}$ = $\Delta C_n/\Delta\delta_{yaw}$, per degree
C_Y = side-force coefficient, side force/qS
C_{Y_β} = side-force parameter, $(\Delta C_Y/\Delta\beta)_{\beta=0 \text{ deg, } 3 \text{ deg}}$
$C_{Y_{\delta_{roll}}}$ = $\Delta C_Y/\Delta\delta_{roll}$, per degree
$C_{Y_{\delta_{yaw}}}$ = $\Delta C_Y/\Delta\delta_{yaw}$, per degree
d = body diameter, 2.600 in.
L/D = lift-drag ratio
ι = reference body length, 2.8167 ft
ι_s = strake length
M = Mach number
q = freestream dynamic pressure, lbf/ft^2
S = reference wing planform area, 0.698965 ft^2
X_{cg}/ι = center-of-gravity location as fraction of model length, measured from nose apex
α = angle of attack, deg
β = angle of sideslip, deg
Γ_{tail} = dihedral angle of tail fins, deg
δ_{pitch} = pitch-control deflection of four tail fins (negative with leading edge down), deg
δ_{roll} = differential deflections for roll control, individual tail fins deflected the indicated amount (positive to provide a clockwise rotation as viewed from rear), deg
δ_{yaw} = yaw-control deflection of four tail fins (negative with leading edge left as viewed from rear), deg

Model Configuration Nomenclature

Aft = baseline longitudinal location of model centerline wing
Mid = centerline aft wing moved forward one body diameter
Fwd = centerline aft wing moved forward two body diameters
High = centerline aft wing moved up 0.375 body diameters
Centerline = baseline vertical location of model aft wing
Low = centerline aft wing moved down 0.375 body diameters
W_s = width of strake

Model Components

S_1 = nose strake, $\iota_s/d = 3.00$, $W_s/d = 0.10$
S_2 = nose-body strake, $\iota_s/d = 5.53$, $W_s/d = 0.10$

Subscripts

max = maximum
trim = trimmed conditions ($C_m = 0$)

Introduction

SUPERSONIC cruise capability requirements for future fighter aircraft will force modifications of existing air-launched weapon systems and eventually will lead to new designs for efficient store carriage and separation. Developing new aircraft weapons integration concepts to meet these requirements will provide a challenge for both airframe and missile designers.

It is suggested in Ref. 1 that for some advanced medium-range missile weapon systems, the monoplanar missile concept with low-profile (reduced tail-fin dihedral angle) quadriform tails is a natural shape for efficient conformal carriage on supersonic-cruise-type aircraft. The low-profile tail concept offers the potential for a more efficient conformal-carriage interface between an aircraft and a missile since the tail surfaces require less space in the vertical plane. One desirable feature of this concept should be a balance between good longitudinal

Presented as Paper 90-0620 at the 28th Aerospace Sciences Meeting, Reno, NV, Jan. 8–11, 1990; received Feb. 2, 1990; revision received May 29, 1990; accepted for publication June 8, 1990.

*Aero-Space Technologist, Supersonic/Hypersonic Aerodynamics Branch, Applied Aerodynamics Division. Senior Member AIAA.

†The aerodynamic coefficient data are referred to the body-axis system except for lift and drag, which are referred to the stability-axis system. The moment reference center was located 20.28 in. aft of the model nose (60.0% of the body length).

and good directional aerodynamic stability and control characteristics.

This paper presents selected results from several wind-tunnel investigations that were conducted to study and evaluate monoplanar circular missile configurations with lower profile tail fins than configurations with conventional-cruciform x tail arrangements like those reported in Refs. 2 and 3. The baseline model configuration in this paper has a centerline aft wing with tail fins in planes inclined 30.0 deg to the horizontal. A complete report of the investigation of the present baseline model that includes wing location and nose-strake effects can be found in Ref. 4. Test results for model configurations with tail fins in planes inclined 22.5 and 45.0 deg to the horizontal are reported in Ref. 5.

In this paper, wind-tunnel test results are used to present and discuss the effects of tail-fin dihedral angle, wing longitudinal and vertical location, and nose-body strakes on the static longitudinal and lateral-directional aerodynamic stability and control characteristics. The tests were conducted in the Langley Unitary Plan Wind Tunnel at Mach numbers of 1.70, 2.16, 2.36, and 2.86. The nominal angle-of-attack range was -3–24 deg at a model roll angle of 0 deg. The nominal angle-of-sideslip range was about -4–6 deg. The test Reynolds number was 2.0×10^6 per foot.

These monoplanar circular missile concept studies provide insight into the potential for improving conformal carriage performance and maneuverability of future air-launched missiles.

Test Facility, Models, and Instrumentation

The tests were conducted in the low Mach number test section of the Langley Unitary Plan Wind Tunnel, which is a variable-pressure, continuous-flow facility described in detail in Ref. 6. The tests were conducted at freestream Mach numbers of 1.70–2.86 at a constant Reynolds number per foot of 2.00×10^6. The nominal angle-of-attack range was -3–24 deg and the nominal angle-of-sideslip range was about -4–6 deg. The model roll angle was 0 deg.

Model details and configuration variables are shown in Fig. 1. The model was a monoplanar low-profile-tail configuration that consisted of a cylindrical body with a pointed tangent-ogive nose, delta wings, and four trapezoidal tail fins. The body had a fineness ratio of 13. The wings and tail fins had slab airfoil cross sections with beveled leading and trailing edges. The four tail fins were deflected to obtain pitch, yaw, and roll control.

The wind-tunnel model was constructed so that the wings could have three centerline longitudinal locations and three aft-wing vertical locations. The centerline-aft-wing model configuration was tested with three different tail-fin arrangements shown in the upper-left corner of Fig. 1b. These arrangements consisted of four tail-fin surfaces in planes inclined 22.5, 30.0, and 45.0 deg to the horizontal. The model configuration with the centerline-aft-wing and the 30-deg tail arrangement is called the baseline-model configuration in this paper. Photographs of this configuration are shown in Fig. 2.

In order to investigate wing/tail spacing effects, tests were conducted with the wing of the baseline model moved forward one and two body diameters. The three wing longitudinal test locations represented wing/tail-fin spacings of 0.62, 1.62, and 2.62 body diameters, which are respectively identified as Aft, Mid, and Fwd in the upper-right corner of Fig. 1b. In addition, by moving the centerline-aft wing of the baseline model up or down 0.375 body diameters while maintaining the same wing span, high-, centerline-, and low-aft-wing configurations were obtained. The low-aft-wing configuration was simply the high-aft-wing configuration inverted, shown in the lower-left corner of Fig. 1b. The baseline-model configuration was also tested with two sets of nose-body strakes, illustrated in the lower-right corner of Fig. 1b. Unless otherwise indicated all model configurations have the centerline-aft-wing and the 30.0-deg dihedral angle tail arrangement with zero control deflection.

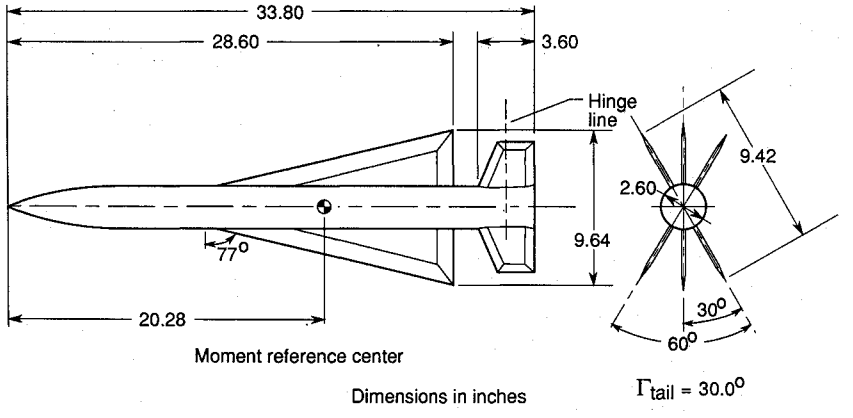

a) Details of baseline-model configuration

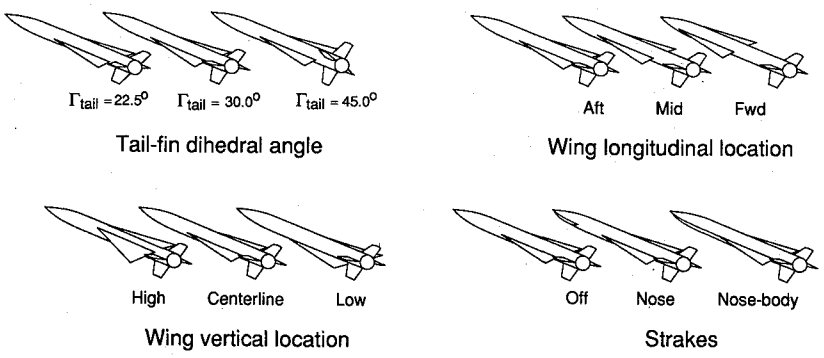

b) Model configuration variables

Fig. 1 Model details and configuration variables.

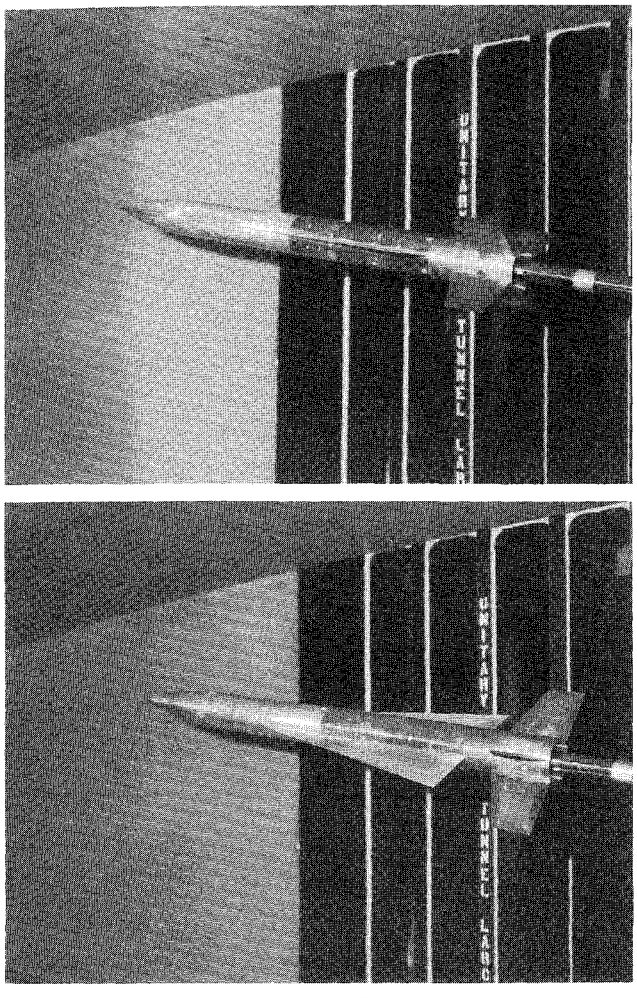

Fig. 2 Photographs of baseline-model configuration.

The dewpoint temperature measured at stagnation pressure was maintained below -30°F to assure negligible condensation effects. All tests were performed with boundary-layer transition strips on the body 1.20 in. aft of the nose and 0.40 in. aft of the leading edges (measured streamwise) on both sides of the wing and tail-fin surfaces. The transition strips were approximately 0.062 in. wide and were composed of No. 50 sand grains sprinkled in acrylic plastic.

Aerodynamic forces and moments on the model were measured by means of a six-component electrical strain-gauge balance housed within the model. The balance was attached to a sting that, in turn, was rigidly fastened to the model support system. Balance-chamber pressure was measured by a single static-pressure orifice located inside of the balance chamber. The model base was feathered to the outer diameter so that no base area existed.

Model angles of attack and sideslip were corrected for deflection of the balance and sting due to aerodynamic loads. Also, angles of attack were corrected for tunnel-flow angularity. The drag coefficient data were adjusted to freestream static pressure acting over the balance chamber exit area at the model base.

Results and Discussion

Longitudinal Aerodynamics

The effect of tail-fin dihedral angle on longitudinal aerodynamic characteristics of the centerline-aft-wing configuration for Mach numbers of 1.70 and 2.86 is presented in Fig. 3. For $M = 1.70$ at the higher angles of attack, increases in tail-fin dihedral angle reduce the lift coefficient and cause a nonlinear increase in pitching moment. The 22.5-deg dihedral tail configuration produces the largest lift coefficient and linear pitching-moment characteristics and provides the most longitudinal stability. The nonlinear variation of pitching moment with angle of attack ($\alpha \approx 8$–14 deg) exhibited by the 45.0 deg dihedral angle tail configuration is characteristic of a monowing missile configuration with a cruciform x tail arrangement at low supersonic Mach numbers.[2,3] For $M = 2.86$, the pitching-moment curves of all the configurations are more linear than those at $M = 1.7$, and the lower profile-tail configurations have slightly higher $(L/D)_{max}$ values.

The effect of wing longitudinal location on longitudinal aerodynamic characteristics of the centerline-wing configurations with the 30.0-deg dihedral angle tail arrangement is presented in Fig. 4. For $M = 1.70$, the forward-wing configuration exhibits the most pitch that coincides with a small loss of lift coefficient at angles of attack 4–10 deg. The pitch nonlinearity is probably due in part to wing-tail interference that results in temporary loss of tail-fin lift since tail-off pitch data (not shown) from Ref. 4 are linear for the test angle-of-attack range. This interference occurs as the tail fins move through the wing downwash flowfield and through the low-energy wake flowfield behind the wing. Another possible contributer to the pitch nonlinearity may be forebody lift. In general, all the wing configurations exhibit some degree of pitch nonlinearity with the forward-wing configuration having the least restoring moments at the higher angles of attack. The mid- and forward-wing configurations produce the largest lift coefficients at the larger angles of attack. At angles of attack above 12 deg, the nonlinear contribution to overall lift for all the wing configurations is primarily due to wing-vortex lift that is characteristic of highly swept and sharp leading-edge wings. At $M = 2.86$, all of the configurations exhibit a reduc-

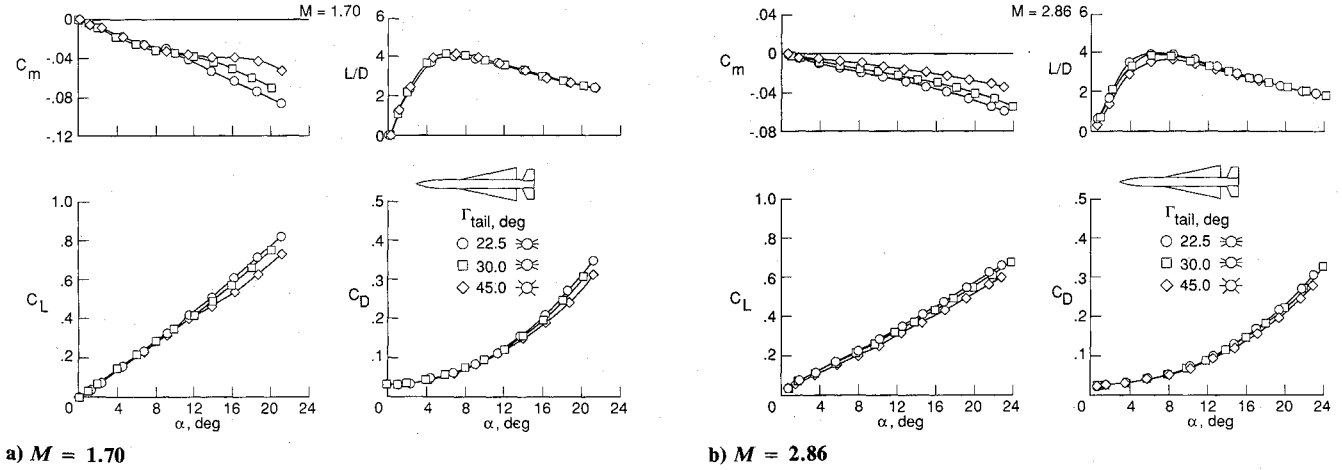

a) $M = 1.70$ b) $M = 2.86$

Fig. 3 Effect of tail-fin dihedral angle on longitudinal characteristics of the centerline-aft-wing configuration.

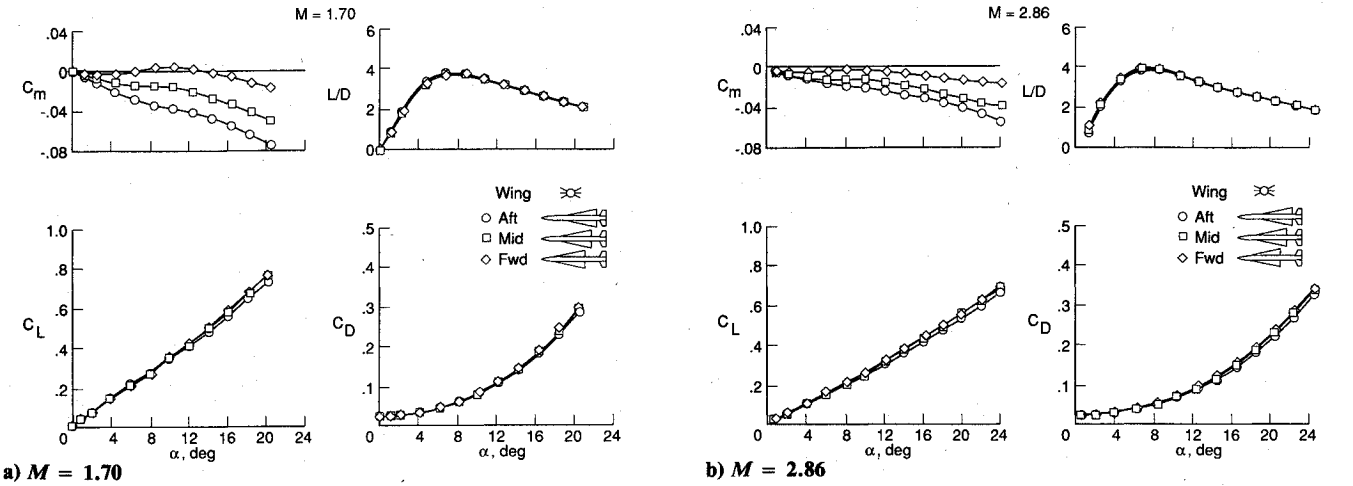

a) $M = 1.70$ b) $M = 2.86$

Fig. 4 Effect of wing longitudinal location on longitudinal characteristics of the centerline-wing configurations; $\Gamma_{tail} = 30.0$ deg.

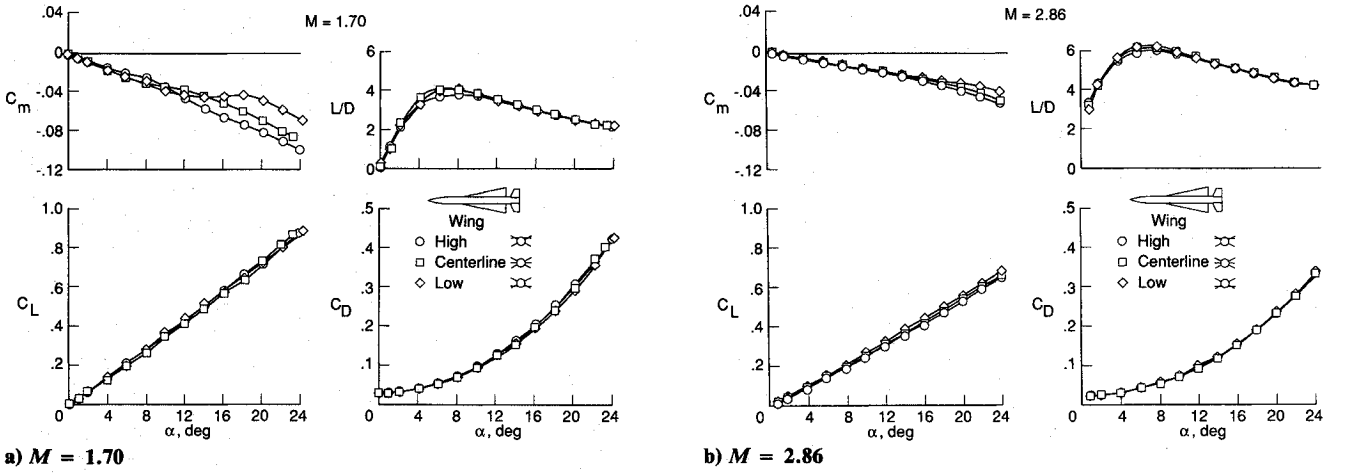

a) $M = 1.70$ b) $M = 2.86$

Fig. 5 Effect of wing vertical location on longitudinal characteristics of the aft-wing configurations; $\Gamma_{tail} = 30.0$ deg.

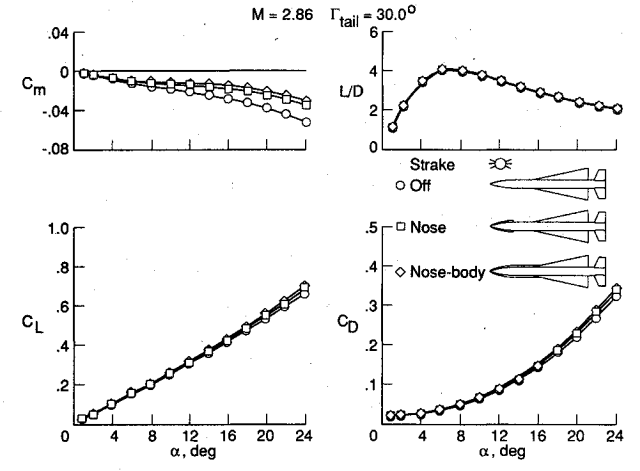

Fig. 6 Effect of strakes on longitudinal characteristics of the baseline-model configuration; $\Gamma_{tail} = 30.0$ deg.

tion in longitudinal stability and nearly linear pitching-moment curves.

The effect of wing vertical location on the longitudinal aerodynamic characteristics of the aft-wing configurations with the 30.0 deg dihedral angle tail arrangement is shown in Fig. 5. The angle of attack at which pitch nonlinearity occurs is strongly related to the wing vertical location. In general, the angle at which pitch nonlinearity begins progressively increases as the wing location is lowered. For example, nonlinearity in pitching moment for the high-, mid-, and low-wing configurations begins at $\alpha \approx 6$, 8, and 12 deg, respectively ($M = 1.70$). The low-wing configuration has the largest nonlinear pitching moment whose magnitude is significantly reduced for $M = 2.86$. Additional tests are needed to resolve the question of whether the upper or lower pair of tail fins is the primary contributor to the pitch nonlinearities. The centerline and low wing configurations have the largest values of $(L/D)_{max}$.

It was suggested in Ref. 5 that for high supersonic Mach numbers the addition of nose-body strakes might provide more directional stability at the high angles of attack for the low-profile tail configurations with $\Gamma_{tail} < 45$ deg. In addition, the anticipated reduction in static margin would result in higher trimmed-lift coefficients and lower trimmed drag. For these reasons, nose-body strakes were investigated on the baseline configuration.

The effect of strakes at $M = 2.86$ on longitudinal aerodynamic characteristics of the baseline configuration is presented in Fig. 6. Both the nose and nose-body strakes provided small increases in lift coefficient at the higher angles of attack and produced the expected reductions in stability level characterized by a small pitch-up tendency ($\alpha \approx 6$–10 deg).

Pitch Control

Pitch control effectiveness, including the effects of tail-fin dihedral angle and wing longitudinal and vertical locations, is presented in Fig. 7. The tail fins of all configurations are effective in producing pitch control and exhibit more effectiveness at $M = 1.70$ than at $M = 2.86$. In general, for each of the configurations the effectiveness value levels were essentially constant over the angle-of-attack range.

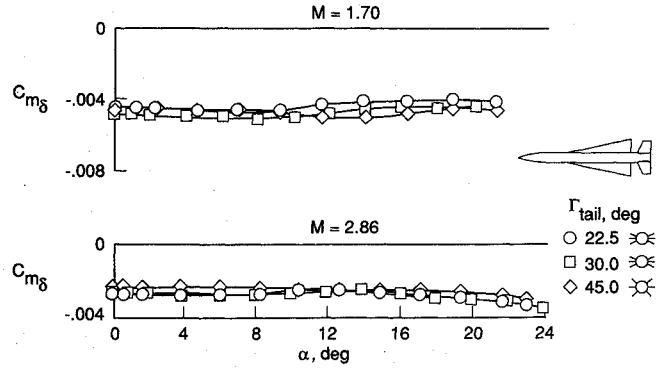

a) Effect of tail-fin dihedral angle; centerline-aft-wing configuration

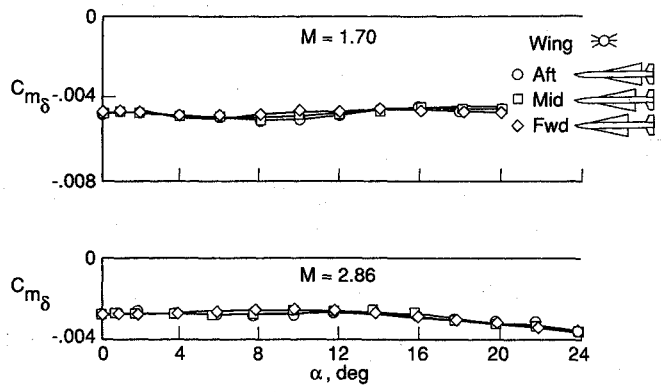

b) Effect of wing longitudinal location, centerline wing; Γ_{tail} = 30.0 deg

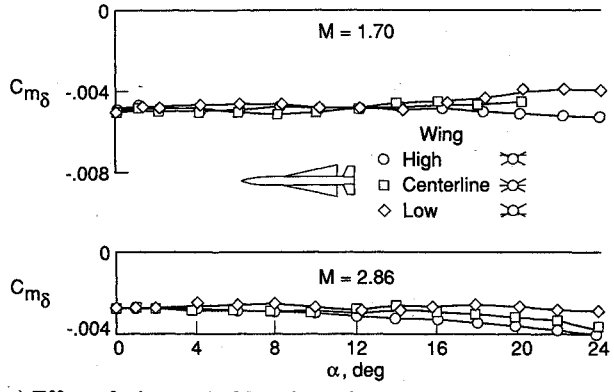

c) Effect of wing vertical location, aft wing; Γ_{tail} = 30.0 deg

Fig. 7 Pitch control effectiveness; $\delta_{pitch} = -10$ deg.

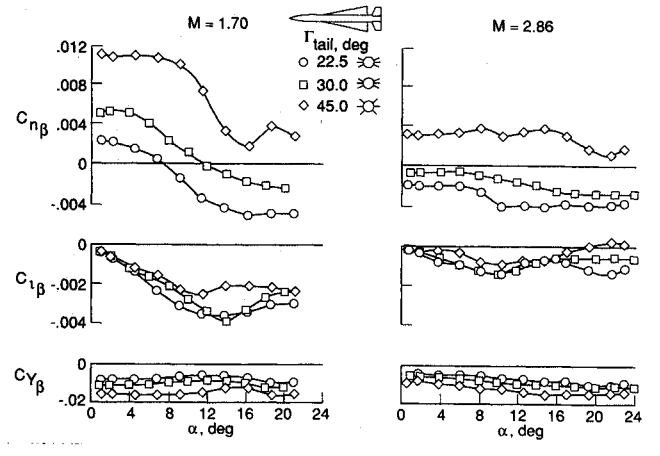

Fig. 8 Effect of tail-fin dihedral angle on the lateral-directional aerodynamic parameters of the centerline-aft-wing configuration.

Lateral-Directional Aerodynamics

The effect of tail-fin dihedral angle on the lateral-directional aerodynamic parameters of the centerline-aft-wing configuration is presented in Fig. 8. For $M = 1.70$, there is a reduction of C_{n_β}, with increases in angle of attack for all three tail arrangements. For the selected moment center (0.60 ι) the lower profile-tail configurations with tail-fin dihedral angles of 22.5 and 30.0 deg become unstable at $\alpha = 8$ and 12 deg, respectively. The cruciform tail configuration ($\Gamma_{tail} = 45.0$ deg) is stable for the entire angle-of-attack range. At $M = 2.86$, only the cruciform tail configuration is stable. The lower profile-tail configurations ($\Gamma_{tail} < 45$ deg) have the most positive effective dihedral ($-C_{\iota_\beta}$).

The effect of wing longitudinal location on lateral-directional parameters of the centerline-wing configurations is shown in Fig. 9. There is a small reduction in C_{n_β} at the lower angles of attack, with increases in wing-tail spacing at $M = 1.70$. This reduction coincides with pitch nonlinearities and loss of lift coefficient ($\alpha \approx 4$–10 deg), as shown in Fig. 4a. The effects of wing longitudinal location on C_{n_β} may be related to forebody lift (and side-force) variations. In general, at the higher angles of attack ($\alpha \geq 10$ deg) there are small increases in C_{n_β} with increased wing-tail spacing. As expected, all the wing configurations are less stable at $M = 2.86$ than at $M = 1.70$. In general, there is an increase in positive effective dihedral parameter ($-C_{\iota_\beta}$) at higher angles of attack, with increases in wing-tail spacing for both Mach numbers of 1.70 and 2.86.

The effect of wing vertical location on lateral-directional parameters of the aft-wing configurations is shown in Fig. 10. The centerline-aft wing ($M = 1.70$) exhibits the most positive C_{n_β} at the lower angles of attack. At intermediate angles (up

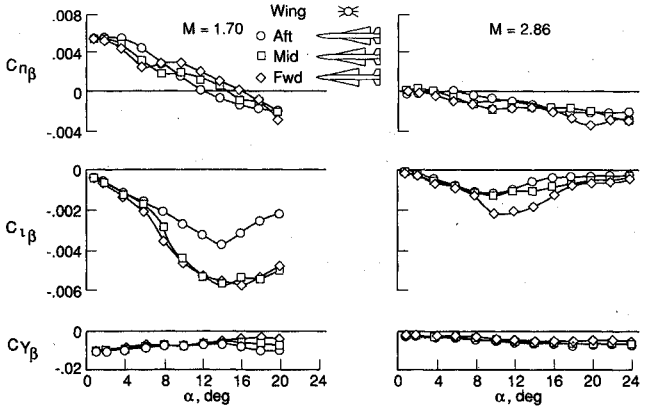

Fig. 9 Effect of wing longitudinal location on lateral-directional parameters of the centerline-wing configurations; Γ_{tail} = 30.0 deg.

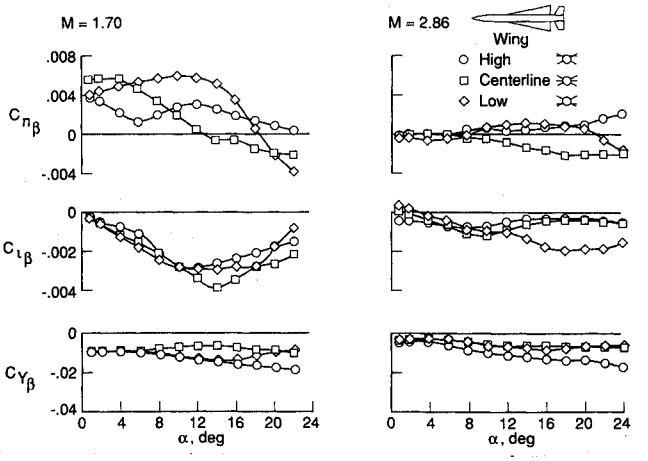

Fig. 10 Effect of wing vertical location on the lateral-directional parameters of the aft-wing configurations; Γ_{tail} = 30.0 deg.

to about 18 deg), the low-wing configuration produces the greatest directional stability. For the higher angles of attack ($\alpha > 18$ deg), the high-wing configuration has the most C_{n_β}. As Mach number is increased to 2.86, all the configurations become less stable at low angles of attack.

Because both of the lower profile tails were unstable at $M = 2.86$, the employment of nose strakes to alleviate this problem was examined. The effect of strake length on lateral-directional parameters of the baseline configuration with zero control deflection is shown in Fig. 11a. Both the nose and

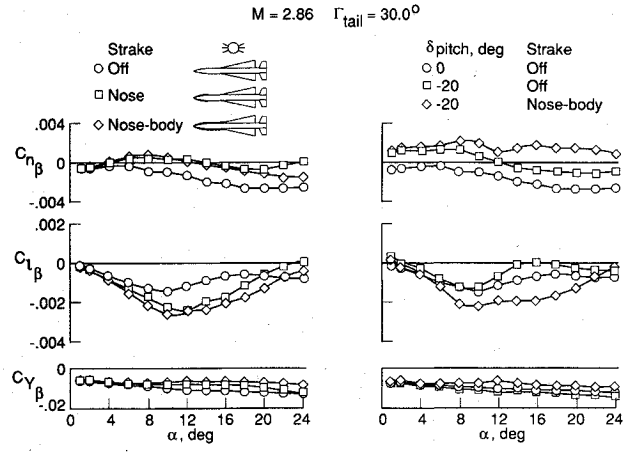

a) Effect of strake length; zero control deflection

b) Effect of nose-body strake and/or pitch control

Fig. 11 Effect of strakes and/or pitch control deflection on lateral-directional parameters of the baseline-model configuration.

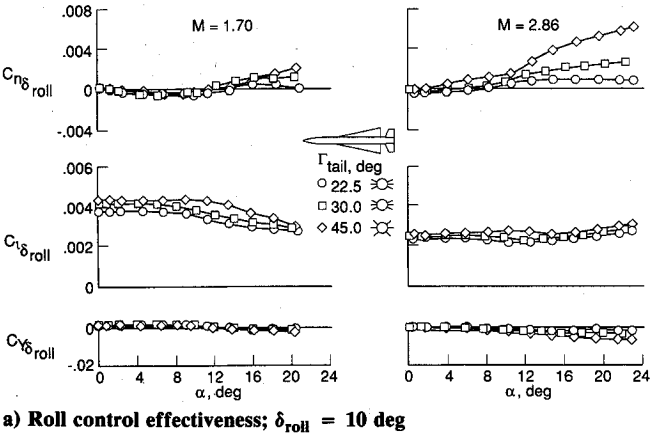

a) Roll control effectiveness; $\delta_{roll} = 10$ deg

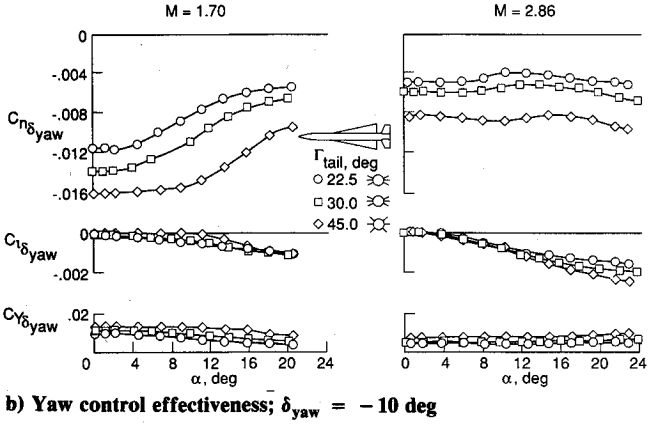

b) Yaw control effectiveness; $\delta_{yaw} = -10$ deg

Fig. 12 Effect of tail-fin dihedral angle on roll and yaw control effectiveness of the centerline-aft-wing configuration.

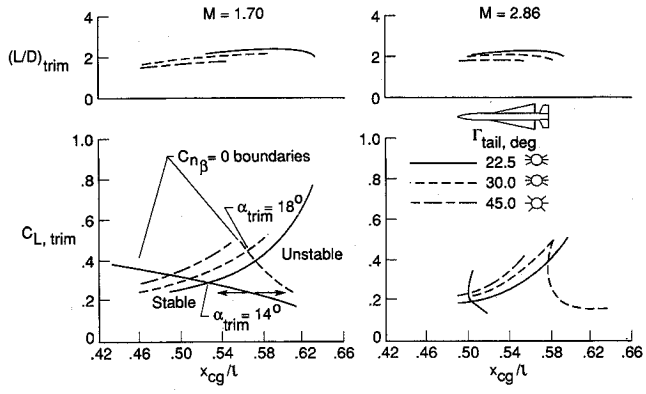

a) Effect of tail-fin dihedral angle, centerline-aft-wing configuration

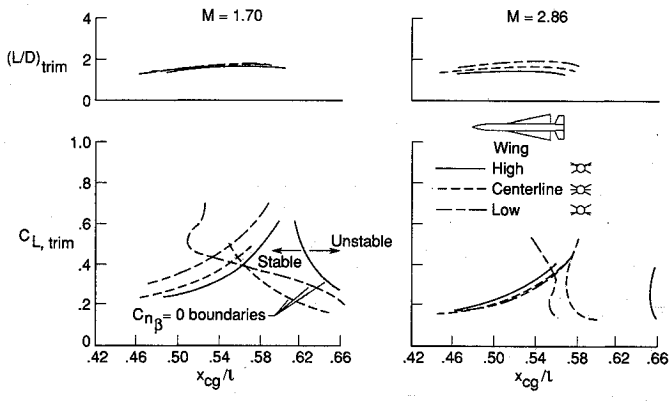

b) Effect of wing vertical location, aft-wing configuration; $\Gamma_{tail} = 30.0$ deg

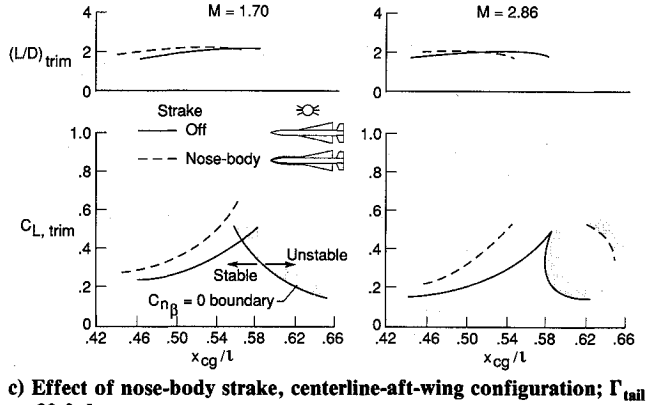

c) Effect of nose-body strake, centerline-aft-wing configuration; $\Gamma_{tail} = 30.0$ deg

Fig. 13 Variation of $C_{L,trim}$ and $(L/D)_{trim}$ with center-of-gravity location; $\delta_{pitch} = -20$ deg.

nose-body strakes increase C_{n_β} at angles of attack above 4 deg. In general, there are increases in positive effective-dihedral parameter ($-C_{l_\beta}$), with increases in strake length. Figure 11b shows the effects of the nose-body strake and/or pitch control ($\delta_{pitch} = -20$ deg) on the lateral-directional parameters of the baseline configuration. The addition of the strake and/or the pitch control provides positive increments of C_{n_β} to the baseline configuration for the entire test angle-of-attack range. The nose-body strake also increases the positive effective dihedral parameter.

Roll and Yaw Control

The effect of tail-fin dihedral angle on roll and yaw control effectiveness of the centerline-aft-wing configuration is presented in Fig. 12. These data were derived from tail-fin deflection angles of -10 deg for yaw control and 10 deg for roll control. In Fig. 12a, all the tail-fin arrangements are effective in producing roll control throughout the angle of attack for M

= 1.70 and 2.86. This roll control is accompanied by favorable yaw at the higher angles of attack for each of the tail-fin configurations. The cruciform tail produced the most roll control and favorable yaw. For the yaw control case (Fig. 12b), each of the tail configurations are effective in providing yaw control that is accompanied by favorable roll at the higher angles of attack. Under some conditions, a fair amount of control is required to correct for yaw-due-to-roll and roll-due-to-yaw.

Trim Characteristics

The balance between good longitudinal and good directional aerodynamic stability and control characteristics is an important consideration when evaluating monoplanar missile configurations. Therefore, when making aerodynamic stability and control comparisons, one must be cognizant of the directional-stability parameter of each configuration in addition to its respective trimmed-lift coefficient. In the following discussion, figures are presented that show variations of trimmed lift coefficient and trimmed lift-drag ratio with center-of-gravity location for selected model configurations. Included are $C_{n_\beta} = 0$ boundary curves that indicate the rearward center-of-gravity limit for the condition of static directional stability. The results are evaluated with the view that a mission is involved for which large turning forces (e.g., pull-ups or a pitch-up maneuver from level flight) are required.

The variation of $C_{L,\text{trim}}$ and $(L/D)_{\text{trim}}$ with center-of-gravity location that includes effects of tail-fin dihedral angle, wing vertical location, and nose-body strake is presented in Fig. 13 for a pitch-control deflection of -20 deg. In each case, the curves were terminated at the highest test angle of attack. In Fig. 13a, the extreme low-profile tail configuration ($\Gamma_{\text{tail}} = 22.5$ deg) is severely limited in $C_{L,\text{trim}}$ (maneuver potential) due to directional instability, especially at the highest test Mach number 2.86. The 30.0 deg dihedral-tail configuration is less limited in maneuver potential and the cruciform-tail configuration ($\Gamma_{\text{tail}} = 45.0$ deg) is unlimited. In Fig. 13b, the high-wing configuration, for the $C_{n_\beta} = 0$ boundary conditions shown, is unlimited and the other wing configurations are limited in maneuver potential. For the center-aft-wing configurations of Fig. 13c, the strake-off configuration has stable maximum $C_{L,\text{trim}}$ values that range from about 0.25 to 0.45 at $M = 1.70$. The addition of the strake increases directional stability that allows stable $C_{L,\text{trim}}$ values for the entire test angle-of-attack range. Addition of the strake also increased $(L/D)_{\text{trim}}$ values for the forward center-of-gravity locations.

Summary and Concluding Remarks

Wind-tunnel tests have been conducted on monoplanar circular missile configurations with low-profile quadriform tail fins to provide an aerodynamic data base to study and evaluate air-launched missile candidates for efficient conformal carriage on supersonic-cruise-type aircraft. The tests were conducted in the NASA Langley Unitary Plan Wind Tunnel at Mach numbers 1.70–2.86 for a constant Reynolds number per foot of 2.00×10^6. Selected test results are presented to show the effects of tail-fin dihedral angle, wing longitudinal and vertical location, and nose-body strakes on the static longitudinal and lateral-directional aerodynamic stability and control characteristics.

The results of the investigation are as follows:

1) The tail fins for each dihedral-angle arrangement tested are effective pitch, roll, and yaw control devices.

2) A reduction in tail-fin dihedral angle reduces nonlinear variations of pitching moment with angle-of-attack and directional stability that limits stable $C_{L,\text{trim}}$ values (maneuver potential).

3) An increase in wing-tail longitudinal spacing promotes nonlinearities in pitching moment and has only small effects on directional stability.

4) A change in wing height (vertical location) strongly influences the angle of attack at which nonlinear pitching moment, maximum directional stability, and the most stable $C_{L,\text{trim}}$ values occur.

5) The addition of nose-body strakes to the baseline configuration increases directional stability, which allows higher stable $C_{L,\text{trim}}$ values.

References

[1]Sawyer, W. C., Jackson, C. M., Jr., and Blair, A. B., Jr., "Aerodynamic Technologies for the Next Generation of Missiles," presented at the AIAA/ADPA Tactical Missile Conf., Gaithersburg, MD, April 27-28, 1977.

[2]Presnell, J. G., Jr., "Investigation of Control Effectiveness and Stability Characteristics of a Model of a Low-Wing Missile with Interdigitated Tail Surfaces at Mach Numbers of 2.29, 2.97, and 3.51," NACA RM L58C19, 1958.

[3]Jernell, L. S., "Stability and Control Characteristics of a Monoplane Missile with Large Delta Wings and Various Tail Controls at Mach 1.90 to 2.86," NASA TM X-71984, 1974.

[4]Blair, A. B., Jr., "Effect of Wing Location and Strakes on Stability and Control Characteristics of a Monoplanar Circular Missile with Low-Profile Tail Fins at Supersonic Speeds," NASA TM-81878, 1980.

[5]Blair, A. B., Jr., "Stability and Control Characteristics of a Monoplanar Missile Configuration with Two Low-Profile Tail Arrangements at Mach Numbers From 1.70 to 2.86," NASA TM X-3533, 1977.

[6]Jackson, C. M., Jr., Corlett, W. A., and Monta, W. J., "Description and Calibration of the Langley Unitary Plan Wind Tunnel," NASA TP-1905, 1981.

Walter B. Sturek
Associate Editor